Dipolar interactions between dangling bonds at the (111) Si-SiO_2 interface

K. L. Brower and T. J. Headley
Sandia National Laboratories, Albuquerque, New Mexico 87185
(Received 24 March 1986)

In this paper a computational model is developed which allows one to calculate the contribution to the Zeeman linewidth arising from magnetic dipole-dipole interactions between unpaired electrons in the dilute limit, which in our specific application correspond to dangling bonds (P_b centers) localized at the (111) Si-SiO_2 interface. Transmission-electron-microscopy studies of the samples we studied with electron paramagnetic resonance (EPR) indicate that the interface between the silicon and the thermally grown oxide was chemically abrupt and atomically flat over distances ranging from 15 to 300 Å. The atomic flatness of the silicon "surface" at the interface was interrupted by steps from one atomic (111) silicon plane to the next. Thus, the dangling bonds observed by EPR are believed to be essentially localized on a two-dimensional plane. The density of dangling bonds is between 3×10^{12} and 5×10^{12} cm^{-2}, which suggests that resolved fine structure might be detectable as well as broadening of the P_b Zeeman resonance. No resolved fine-structure spectra due to interacting close pairs of dangling bonds are detected in our EPR measurements. This may be due to the effects of isotropic exchange interactions which result in the pair being in the spin singlet state. Another possibility is that the distribution of dangling bonds is not random at the interface but arranged so that the distance between P_b centers is enhanced. Attempts to characterize the dipolar contribution to broadening of the Zeeman resonance in terms of even moments using the method developed by Van Vleck proves to be inadequate. Consequently, the dipolar contribution to the P_b Zeeman resonance is calculated by adding the hypothetical EPR spectra from 1-, 2-, . . . , 6-electron systems assuming only magnetic dipole-dipole interactions between the spins and weighted in proportion to their statistical probability of ocurrence. The contribution to the total linewidth of the P_b Zeeman spectrum, which is 2.1 G (full width at half maximum), is calculated to be about 0.35 G for the case in which the applied magnetic field is perpendicular to the (111) Si-SiO_2 interface.

I. INTRODUCTION

Transmission-electron-microscopy (TEM) studies of the (111) Si-SiO_2 interface indicate that the crystalline silicon surface of the interface can be abrupt and atomically flat over long distances.[1,2] In such cases the flatness of the interface is interrupted by steps, called ledges, which are typically 1 or 2 atomic steps (3.14 Å) high and up to several hundred angstroms apart.[2] It is interesting that a solid-solid interface can grow so perfectly flat. Mazur and Washburn have proposed on the basis of their TEM studies of singular (111), vicinal (111) 3° [$1\bar{1}0$], and (111) 2° [$11\bar{2}$] silicon-oxidized surfaces that oxidation proceeds rapidly at ledges.[3] Such a mechanism would tend to plane the silicon surface atomically flat. If the distance between ledges from which oxidation proceeds becomes too great, it appears to become energetically favorable for a new ledge to be generated. Ponce and Yamashita have also observed abrupt and atomically flat interfaces between crystalline silicon and embedded SiO_2 precipitates that grow in oxygen-doped silicon at 1200 °C.[4] In this case the geometry of the polyhedral SiO_2 precipitate matches that resulting from minimizing the interfacial strain energy. The silicon matrix surrounding the precipitate is observed by TEM to be virtually strain-free.

Electron paramagnetic resonance (EPR) studies have identified various features in the structure of a dangling-bond defect at the (111) Si-SiO_2 interface.[5–8] This defect, which is referred to as the P_b center, is shown schematically in Fig. 1. It is also the dominant defect responsible for charge trapping at the interface.[9,10] The surface density of P_b centers observed from dry thermal oxides grown on polished (111) silicon surfaces is typically several times 10^{12} cm^{-2}.[5,6] Thus approximately 0.5% of the [111] Si bonding sites are occupied by a dangling bond. A planar spin density of this magnitude suggests the possibility that resolved satellite spectra due to unpaired electrons interacting via magnetic dipole-dipole interactions might be observable. In addition, the interactions between these spins might also affect the linewidth and line shape of the Zeeman resonance. If the effects due to dipolar interactions could be detected, then one might be able to infer something about the distribution of spins on this essentially two-dimensional atomic plane as well as perhaps information which would contribute to some understanding of the physical mechanism(s) by which these paramagnetic defects are produced at the interface.

We have previously made a detailed study of the angular variation in the linewidth of the Zeeman P_b resonance associated with dangling bonds at the (111) Si-SiO_2 interface.[8,11] Although there is a distinct variation in the linewidth as a function of the direction of the applied magnetic field, we have shown this to be due to the effects of strain on the $\overleftrightarrow{g}$ dyadic. Although the angular variation in the linewidth due to electronic dipolar effects is distinct and different from that due to the strain broadening of the dangling-bond resonance, we have as of yet been un-

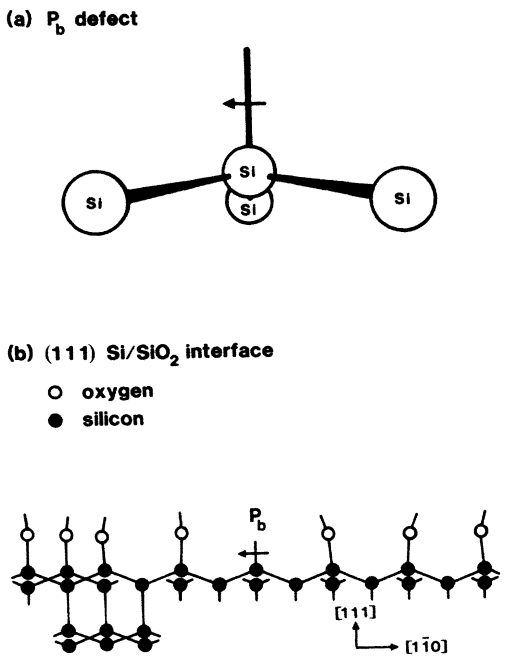

FIG. 1. (a) Basic paramagnetic unit giving rise to the P_b resonance. The paramagnetism arises from an unpaired electron localized in a dangling Si hybrid orbital (arrow) on a Si atom which is covalently bonded to the three lower silicon atoms. This defect has C_{3v} symmetry. (b) Context in which the basic paramagnetic unit is presently believed to exist. The essential features in this schematic are that the (111) $Si-SiO_2$ interface can be atomically abrupt and flat over long distances, oxygen atoms of the vitreous silica are ordinarily bonded to the [111] Si bonds at the interface, and P_b centers exist where an oxygen atom is not bonded to a surface crystalline silicon atom. The bonding of the oxygen atoms in turn to atoms within the vitreous oxide is not shown in this schematic (the truncated oxygen bonds). The ordered silicon atoms represent the bulk crystalline silicon as seen looking along a [11$\bar{2}$] direction.

able to detect any line broadening due to dipolar effects. On the other hand, calculations of the linewidth deduced from just the second moment for a random distribution of spins localized at [111] Si bonding sites suggest that dipolar broadening ought to be observable.[11] This apparent discrepancy between experiment and one theoretical aspect of the problem has prompted us to investigate this effect more carefully.

In this paper we first present the results of pertinent EPR studies and TEM measurements which closely define the actual material environment on an atomic scale (Sec. II). The study of the effects of magnetic dipole-dipole interactions between dangling bonds divides into two parts. One part deals with the effects of dipolar interactions between close pairs which are expected to give resolved fine-structure spectra (Sec. III A), and the other deals with the effects of dipolar interactions which are expected to contribute to the broadening of the P_b Zeeman resonance. Two methods are considered for determining the dipolar effects on the broadening of the Zeeman resonance: The first method considers the method of moments first developed by Van Vleck (Sec. III B), and the second method is based on a computational model (Sec. III C). Our conclusions are presented in Sec. IV.

II. EXPERIMENTAL RESULTS

The Zeeman resonance due to dangling bonds at the (111) $Si-SiO_2$ interface for the applied magnetic field **B** perpendicular to the interface (**B**||[111]) is shown in Fig. 2. This spectrum was observed with a *K*-band superheterodyne spectrometer in the absorption mode under conditions of slow passage. Since phase-sensitive detection was used to detect the magnetic field modulated resonance, the recorded spectrum in Fig. 2(a) is the derivative of its absorption resonance which is shown in Fig. 2(b). The absorption resonance was obtained by computational numerical integration of the derivative spectrum. The derivative spectrum is, in fact, the same one as shown in Fig. 2(b) for $\theta=0$ of Ref. 8, and of course is from the same sample as studied previously. The conditions under which these EPR measurements were made have been presented in considerable detail previously.[8]

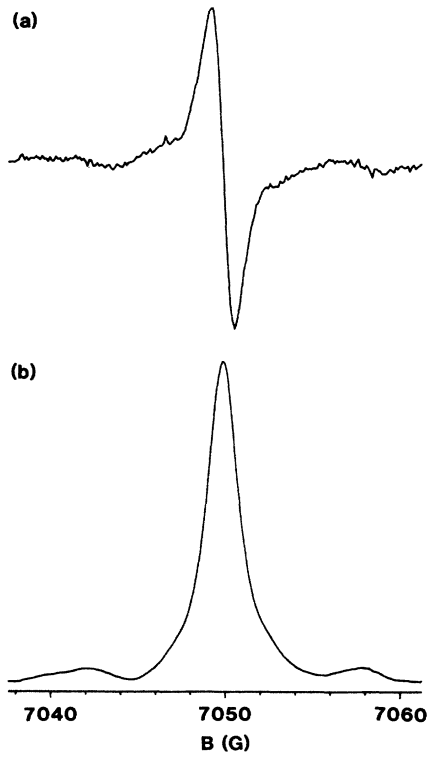

FIG. 2. (a) Derivative P_b Zeeman spectrum observed in the absorption mode using narrow band lock-in detection under conditions of slow passage for **B**||[111] direction [**B** perpendicular to the (111) interface]. This spectrum was measured at 100 K with a microwave frequency of 19.752 GHz. (b) Integral P_b spectrum obtained by numerical integration of the derivative spectrum.

Extensive analysis of the line shape of this particular resonance has been made previously[8] and shows that it is well represented by the Voigt function, which is a convolution of Gaussian and Lorentzian line broadening. In the case of this particular spectrum the total peak-to-peak derivative linewidth ΔB_{pp}^{T} is 1.33 G. The peak-to-peak Gaussian component, ΔB_{pp}^{G} is 0.49 G and the peak-to-peak Lorentzian component ΔB_{pp}^{L} is 1.14 G. One of the important aspects of the spectrum shown in Fig. 2 is that for this direction of the magnetic field no contribution to line broadening due to strain, at least to first order, is expected.[8] Thus the broadening of this resonance is believed to be due primarily to ^{29}Si hyperfine broadening and possibly electronic dipolar broadening. The pair of satellite lines on either side of the Zeeman line in Fig. 2 is believed to be due to ^{29}Si superhyperfine interactions with a distinct set of neighboring Si atoms within the silicon. This satellite structure is commonly observed in the spectra of isolated deep-level defects in silicon. However, in this work we also show that similar satellite spectra due to pairs of P_b centers may (or may not) also be possible. Finally, the other important aspect pertaining to dipolar effects concerns the planar density of unpaired spins. The resonance in Fig. 2 corresponds to between 3×10^{12} and 5×10^{12} P_b centers cm^{-2}.[8]

This particular sample bundle is in fact the same one that was used in our ^{29}Si hyperfine studies of the P_b center[7] as well as in our studies of the strain broadening of the P_b spectrum.[8] A detailed description of the experimental conditions under which these thermal oxides on silicon were prepared has been presented previously.[7,8] In particular, this dry oxide was grown at 900 °C in dry oxygen at a pressure of 1.2×10^{5} Pa to a thickness of 2300 Å.

In addition to the EPR measurements which we have performed on this set of samples, we have also recently examined this interface with TEM. The samples used for the TEM measurements were randomly selected from the remaining samples in the original group which were thermally oxidized at the same time. The importance of these TEM measurements is that they characterize the flatness of the Si-SiO_2 interface in samples taken from the same group on which extensive EPR measurements presented here and elsewhere[7,8] have been made.

Specimens for cross-sectional electron microscopy were prepared by epoxying two wafers together with the oxide surfaces face-to-face. Cross sections through the sandwich were cut on a diamond saw, ground to a thickness of approximately 75 μm, polished on both sides with 1-μm diamond paste, and ion-milled to perforation. High-resolution electron microscopy of the Si-SiO_2 interface was performed in a JEM-200CX electron microscope operating at 200 keV. Two-beam lattice images using tilted illumination were obtained from the set of {111} planes (0.34-nm spacing) parallel to the silicon wafer surface. Figure 3 is a typical high-resolution image of the Si-SiO_2 interface showing (111) lattice fringes parallel to the interface. The interface was found to be flat to within 2 (111)-plane spacings over long distances. Atomic steps at the interface, imaged as terminations of fringes (arrows), range in spacing from 15 to 300 Å with an average step spacing of $\approx$110 Å over long distances.

FIG. 3. Transmission electron microscopy view of the (111) Si-SiO_2 interface on samples selected at random from the original group from which other samples had been selected for EPR measurements. The samples in the "original group" were all thermally oxidized at the same time. The arrows indicate the positions of ledges or steps at the interface.

III. EFFECTS OF DIPOLAR INTERACTIONS BETWEEN ELECTRON SPINS

A. Resolved fine-structure splittings

The fine-structure spectrum for a pair of interacting spins is described by the spin Hamiltonian

$$\mathcal{H}=\mu_B \mathbf{B}\cdot\vec{g}\cdot(\mathbf{S}_i+\mathbf{S}_j)+J_{ij}\mathbf{S}_i\cdot\mathbf{S}_j+\mathbf{S}_i\cdot\vec{D}_{ij}\cdot\mathbf{S}_j\ , \qquad (1)$$

where Tr $(\vec{D}_{ij})=0$. The isotropic exchange interaction, $J_{ij}\mathbf{S}_i\cdot\mathbf{S}_j$, gives the splitting between the singlet and the triplet states, and the splittings among the triplet states are dictated by the (symmetric) anisotropic spin-spin interaction $\mathbf{S}_i\cdot\vec{D}_{ij}\cdot\mathbf{S}_j$. The allowed EPR transitions occur between the triplet states and give rise to two resonances, called the fine-structure spectrum; the magnetic field separation between these two resonances will be referred to as the fine-structure splitting.

We see no evidence that the P_b Zeeman resonance is exchanged narrowed. In fact, the existence of partially resolved satellite structure on the shoulders of the Zeeman resonance indicates that it is not exchange narrowed. Therefore, the amount of overlap of the paramagnetic wave functions is too small to cause significant exchange narrowing effects. This is consistent with the overall aspects of the defect model; EPR measurements of the ^{29}Si hyperfine interaction indicate that 80% of the unpaired spin density is localized on the trivalent bonded Si atom.[7] Since the planar density of P_b centers is $(3-5)\times10^{12}$ cm^{-2} giving a mean separation between P_b centers of about 50 Å, the average exchange interaction arising from overlap would appear to be very small.

Previous studies indicate that in the case of spin 1 multiple vacancy (oxygen) defects in silicon and diamond, the anisotropic spin-spin interaction is dominated by the magnetic dipole-dipole interaction.[12–14] This is also true for the neutral 1-vacancy-oxygen center in silicon where the dangling bonds are mostly localized on two silicon atoms only 3.8-Å apart.[15] In cases where the two unpaired elec-

trons are both highly localized within the same space, the spin-spin interaction can be dominated by other interactions.[16] For close spin pairs where the difference in energy between the triplet and singlet states is much greater than kT and J is greater than zero, the defect pair will be in a diamagnetic spin-singlet state.

It is possible to calculate the fine-structure splittings for the case in which the anisotropic spin-spin interaction is dominated by the magnetic dipole-dipole interaction. For close pairs such as multiple (oxygen) vacancy spin 1 defects, fine-structure splittings can be accurately calculated by assuming a wave function with localization and s and p character as deduced from ^{29}Si hyperfine measurements.[12,15] The calculation of the magnetic dipole-dipole matrix elements used to determine $\vec{\vec{D}}_{ij}$ is a time-consuming computer computation. For more distant spin pairs, the magnetic dipole-dipole matrix elements may be obtained very easily by assuming a point dipole-dipole interaction with the spin densities totally localized at particular "point defects" (the wave functions being represented by delta functions). One can also estimate the fine-structure splitting for close spin pairs using this approximation as well. In this case the magnetic dipole-dipole interaction is estimated by assuming a point dipole moment at each point defect proportional to the measured spin density localized on only that dangling-bond site—the spin density localized on all other neighboring atomic sites being neglected. This rescaling of the dipolar interactions in this approximate manner for close pairs is reasonable since the magnetic dipole-dipole interaction is proportional to $1/r^3$ and contributions to the matrix elements from the neighboring atomic sites, which are spatially spread out, are ignored.[12]

A schematic diagram of the unreconstructed (111) Si surface showing the [111] sites where the Si is ordinarily bonded to an oxygen atom (solid dots) is illustrated in Fig. 4; the occasional presence of an oxygen vacancy is symbolized by the solid triangle. The presence of other kinds of interface defects (e.g., ledges) is not included in this schematic. The remaining bond intersections are Si atoms bonded to the underlying Si atoms of the silicon crystal.

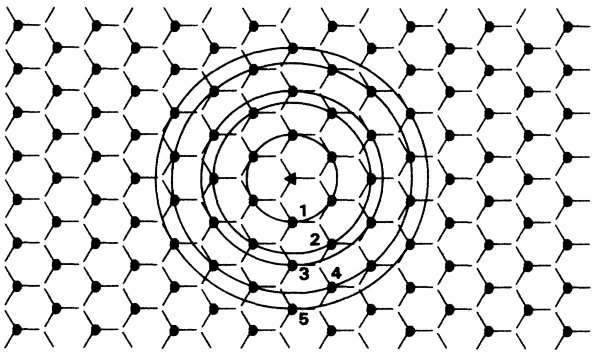

FIG. 4. Top view of the unreconstructed (111) Si surface atoms (●) which can bond to oxygen atoms above this plane forming a (111) Si-SiO_2 interface. The remaining bond intersections are Si atoms bonded to the underlying Si atoms of the crystalline silicon (see Fig. 1 for side view). The circles identify first nearest neighbor (1), second nearest neighbor (2), etc., sites relative to a [111] dangling bond defect (▲). The density of Si-O bonding sites is 7.841×10^{14} cm^{-2}; the separation between Si-O bonding sites is 3.84 Å.

For the case in which **B** is perpendicular to this (111) Si plane, the fine-structure splitting for all pair configurations with one unpaired spin at the center and the other unpaired spin in any site within a given shell is degenerate by symmetry. The fine-structure splitting for **B** perpendicular to the (111) Si-SiO_2 interface is plotted in Fig. 5 for the 5 nearest-neighbor (NN) pair configurations. It is expected that fine-structure splittings >15 G should be well resolved; this is expected to include the 1NN, 2NN, and 3NN pairs. Fine-structure splittings between approximately 15 and 8 G might be only partially resolved and are expected to arise from 4NN and 5NN pairs. Fine-structure splittings <8 G will most likely be unresolved and should contribute to the dipolar broadening of the Zeeman resonance (see Secs. III B and III C).

Although we have searched for well-resolved fine-structure spectra, with and without light illumination, at sensitivities sufficient for observing pair spectra assuming a random, planar distribution of P_b centers, we have not been able to detect any resolved fine-structure spectra. Three possible explanations which could account for this observation are the following: (1) Isotropic exchange interactions for close pairs of P_b centers result in the pair being in a spin-singlet state. (2) The planar distribution of P_b centers on the (111) Si-SiO_2 interface is not random but instead is such that the separation between dangling

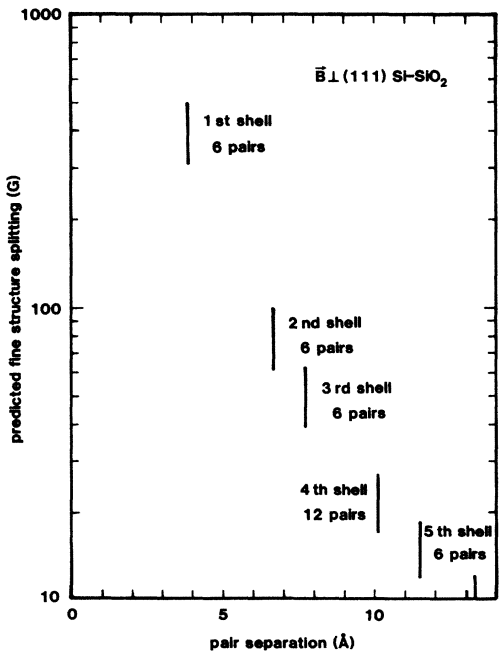

FIG. 5. Predicted fine-structure splittings for the first five nearest-neighbor pairs as function of the pair separation. The range of fine-structure splittings is represented by the vertical bars resulting from a point-dipole calculation in which the spin density ranges from 100 (maximum splitting) to 75 %.

bonds tends to be enhanced. Such a distribution might occur if dangling bonds are produced as a result of the release of strain energy from finite regions of the interface during the cool-down period after thermal oxidation. (3) The P_b centers are not confined to a plane but distributed in depth as well. In the case of the (111) Si-SiO_2 interface, all models of the P_b center involve a dangling-bond localized on a "surface" silicon atom adjacent to the oxide. No suitable model for a defect embedded within the bulk silicon very near to the interface having the correct symmetry and preferred orientation consistent with all the presently known EPR data has yet been devised. Until such a defect model is devised, this alternative is untenable.

B. Method of moments

Van Vleck has shown how the absorption resonance due to magnetic dipole transitions between energy levels split by the Zeeman, exchange, and dipolar interactions can be represented in terms of moments.[17] For the case in which n spins are randomly distributed among N lattice sites and the exchange terms are neglected,[18] the second and fourth moments of the absorption resonance for $n < N$ are the following:

$$\langle(\Delta\nu)^2\rangle_{\rm av}=\frac{S(S+1)}{3h^2}T_{21}f \tag{2}$$

and

$$\langle(\Delta\nu)^4\rangle_{\rm av}=\left[\frac{S(S+1)}{3h^2}\right]^2(T_{41}f+T_{42}f^2)\,, \tag{3}$$

respectively. In Eqs. (2) and (3), f is the fractional site occupancy (n/N). The T_{pq} terms are given by the formulas

$$T_{21}=\sum_k{}' B_{jk}^2\,, \tag{2'}$$

$$T_{41}=\frac{1}{5}\left[7-\frac{3}{2S(S+1)}\right]\sum_k{}' B_{jk}^4\,, \tag{3a}$$

and

$$T_{42}=\sum_{\substack{k,l\\ j\neq k\neq l\neq j}}[3B_{jk}^2B_{jl}^2-\tfrac{4}{9}B_{jk}^2(B_{jl}-B_{kl})^2 +\tfrac{2}{9}B_{jk}B_{kl}(B_{jl}-B_{jk})(B_{jl}-B_{kl})]\,. \tag{3b}$$

The indices k and l in Eqs. (2'), (3a), and (3b) run over the lattice sites but omit the spin site j. The dipolar term B_{jk} is given by the expression

$$B_{jk}=\frac{3\mu_B^2g^2}{2r_{jk}^3}(1-3\cos^2\gamma_{jk})\,, \tag{4}$$

where γ_{jk} is the angle between the direction of the applied magnetic field and $\mathbf{r}_{jk}$, the distance vector from site j to site k. Van Vleck showed that the isotropic exchange interactions do not contribute to the second moment; however, they do contribute to the fourth moment. The contribution of the exchange terms to the fourth moment can be responsible for a narrowing of the resonance line shape that commonly occurs in high spin-density systems. Because the exchange interactions are usually short range, they may be negligible for sufficiently dilute spin systems.

The fourth moment is important since it begins to give information about the line shape which in turn dictates the peak-to-peak derivative linewidth which is commonly used by the experimentalist to characterize line-broadening effects. The fourth moment can be expressed in terms of the square of the second moment as determined from Eqs. (2) and (3) by the expression

$$\langle\Delta\nu^4\rangle_{\rm av}=[\langle(\Delta\nu)^2\rangle_{\rm av}]^2T_{21}^{-2}(T_{42}+T_{41}f^{-1}) \tag{5}$$

which shows that the line shape is dependent on f.[18] In particular, Eq. (5) indicates that as f decreases the fourth moment increases relative to the second moment which would cause the line shape to become more Lorentzian-like. For a Gaussian line shape the term $T_{21}^{-2}(T_{42}+T_{41}f^{-1})$ is equal to 3.

The observed peak-to-peak derivative linewidth of the P_b resonance for **B** perpendicular to the (111) interface is only 1.3 G. As pointed out earlier (Sec. III A), the fine-structure splittings due to magnetic dipole-dipole interactions between just two electrons do not contribute to the line shape of the narrow Zeeman resonance unless the distance between spins exceeds about 13 Å. Contributions to the second moment of the unresolved Zeeman resonance arising from these distant dipolar and unresolved satellite lines can be calculated from Eq. (2) by summing over only sites beyond r_0. If one assumes a Gaussian line shape, then the Gaussian peak-to-peak derivative linewidth ΔB_{pp}^G, as deduced from the second moment, exhibits an angular variation as a function of the magnetic field direction that is shown in Fig. 6. This plot also shows the dependence on the exclusion radius r_0 and the surface density of spins.

However, in calculating the fourth moment, we do not want to include contributions which are associated with resolved fine-structure lines. Unfortunately, the method of including in the sums for the fourth moment only sites outside of the exclusion region around each site is incorrect. Why is this incorrect? At least one problem is

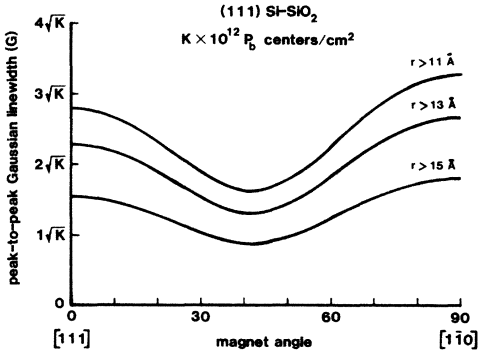

FIG. 6. Calculated peak-to-peak derivative Gaussian linewidth of a dipolar broadened resonance as a function of magnetic field direction as deduced from the second moment. Only pairs with a separation greater than r_0 are included in the evaluation of the summation in Eq. (2). The spin density is expressed as $K\times10^{12}$ cm^{-2} where $K^{1/2}$ is also a scaling factor on the vertical axis.

that Eq. (3) indicates that the fourth moment is based on lattice sums involving two and three spins. The EPR spectrum of a three-electron system is dominated by three intense resonances, one of which is always located at the position of the Zeeman line and the other two appearing as low- and high-field satellites—either resolved or unresolved depending upon the strength of the spin-spin interaction [see, for example, Figs. 7(c), 7(e), 7(h), and 7(i)]. Consequently, it is impossible to distinguish in the summation to the fourth moment between contributions to the resolved and unresolved portions of the spectrum. Thus the functional dependence of the line shape on f in Eq. (5) for our particular problem remains unknown.

EPR measurements and computer analysis of the observed variation in the linewidth of the P_b Zeeman resonance, arising from the (111) Si-SiO_2 interface, as a function of the direction of the applied magnetic field have failed to detect any component in angular variation such as that shown in Fig. 6.[8,11] Furthermore, the peak-to-peak linewidth for **B** perpendicular to the interface for a planar spin density of $(3-5)\times 10^{12}$ spins/cm^2, which corresponds to a K value in Fig. 6 of 3—5, due to electronic dipolar broadening alone is expected to be 2.6 G. This is significantly larger than the 1.3 G peak-to-peak linewidth observed experimentally (see Fig. 2) which includes ^{29}Si hyperfine broadening! The limitations and uncertainties in the method of moments when applied to a problem of this nature has prompted us to consider another approach which is presented in Sec. III C.

C. Computational approach

We now present a computational method for calculating the electronic dipolar broadening of the P_b Zeeman resonance. We will first develop the ideas underlying this computational approach, and then we will present the results and compare them with our experimental observations.

The approach is simply to accumulate a spectrum by calculating the resonant frequencies and amplitudes for all possible, or else a random selection of, spatial configurations of interacting 1-, 2-, ..., p-electron systems contained within a finite region. The accumulated spectra for each of the m-electron systems are subsequently added together in proportion to their statistical probability of occurrence, which is a function of the fractional site occupancy f, to give the total electronic dipolar broadened spectrum. This dipolar spectrum can be subsequently convoluted with other functions representing other sources of line broadening to give the overall line shape. This approach is similar to that used to calculate glass spectra.

The spin Hamiltonian we employ for a dilute distribution of unpaired electrons associated with P_b defects on the (111) Si-SiO_2 interface in the presence of an applied magnetic field **B** is the following:

$$\mathcal{H}=\sum_i \mu_B \mathbf{B}\cdot\overleftrightarrow{g}\cdot\mathbf{S}_i+\sum_{\substack{(i,j)\\ i<j}} J_{ij}\mathbf{S}_i\cdot\mathbf{S}_j + \sum_{\substack{(i,j)\\ i<j}} \mathbf{S}_i\cdot\overleftrightarrow{D}_{ij}\cdot\mathbf{S}_j \ . \tag{6}$$

Our computations were restricted to the case in which **B** is perpendicular to the (111) Si-SiO_2 interface, exchange interactions are neglected, and the anisotropic spin-spin interactions are dominated by magnetic dipole-dipole interactions. Implicit in the numerical determination of the $\overleftrightarrow{D}_{ij}$ is the assumption that the wave function for an unpaired spin, whose actual localization is characteristic of deep-level defects in silicon, is represented by a delta function (point dipole approximation) and that the spins are distinguishable (symmetrization of the space and spin parts of the wave function are unnecessary). Although possible effects due to exchange interactions for close pairs are not included, at least part of the contributions due to close pairs would be associated with the resolved fine-structure spectra. As the distance between spins increases, the point-dipole approximation becomes more acceptable. The effects of ^{29}Si hyperfine interactions on the line shape are considered later.

The eigenvalues E_k and eigenvectors, $|k\rangle$, associated with a specific m-electron configuration are determined by numerical diagonalization of a $2^m\times 2^m$ complex Hermitian matrix. For the special case in which **B** is perpendicular to the plane containing the unpaired spins, this $2^m\times 2^m$ matrix can be reduced to two $(2^m)/2\times(2^m)/2$ complex Hermitian matrices by proper ordering of the rows and columns. The basis spin states used in calculating these matrix elements from the spin Hamiltonian in Eq. (6) are of the form $|S_1, S_2, ..., S_m, M_1, M_2, ..., M_m\rangle$.

The resonant frequencies are specified by the condition

$$h\nu_0=|E_k-E_l| \ . \tag{7}$$

The absolute intensity and frequency dependence of an absorption resonance due to a magnetic dipole transition between eigenstates $|k\rangle$ and $|l\rangle$ of a particular spatial configuration of unpaired spins is the following:[19]

$$P_{kl}(\nu)=\frac{(\pi\mu_B g_t B_t \nu)^2\left|\langle k|\sum_i S_{ti}|l\rangle\right|^2 g_{kl}(\nu)}{\eta_L kT} \ . \tag{8}$$

The intrinsic absorption line shape is defined by the function $g_{kl}(\nu)$, which is a δ function $\delta(\nu-\nu_0)$ for our purposes here; ν is the microwave frequency. The other parameters are B_t, the amplitude of the microwave magnetic field which is perpendicular to the applied magnetic field **B** in Eq. (6); g_t, which is that component of the $\overleftrightarrow{g}$ dyadic parallel to B_t; and S_{ti}, the ith spin operator parallel to B_t. In calculating the transition probabilities, B_t was taken as being parallel to the $[1\bar{1}0]$ direction. Included is the temperature dependence, where $h\nu \ll kT$, and the number of energy levels is n_L, which is related to the total spin of the m-electron system.

In our computer algorithm the relative intensities are accumulated in an array whose index is related to the resonant frequency; this array then represents a histogram of the resolved and unresolved fine-structure spectrum in frequency space. In our computer computations,[20] the index for this array spanned from -2000 to 2000 over an effective magnetic field interval of 20 G centered about the unperturbed Zeeman resonance which was arbitrarily chosen to be 7000 G. Hence, the resolution in this primi-

tive fine-structure spectrum corresponds to 0.005 G. The histograms for the six different m-electron systems are shown in Fig. 7; the horizontal axis has been transformed from frequency to magnetic field for ease of comparison with experimental spectra.[21]

The m-electron configurations of importance correspond to m unpaired electrons occupying the potential Si-O bonding sites shown in Fig. 4 which are contained within a circular region of diameter $d_{\max}$. The diameter of this circular region is chosen such that

$$d_{\max} \cong \left[\frac{\mu_B g}{\delta B}\right]^{1/3}, \tag{9}$$

where δB is the minimum separation in the fine-structure lines in the center of the Zeeman line. In choosing $d_{\max}$, δB should be small compared with other sources of line broadening which are later convoluted with the dipolar histogram. The region in the center of the dipolar-broadened Zeeman line for a two-electron system is illustrated in Fig. 7(g). In our case, $d_{\max}$ is 100 Å which corresponds to a δB of approximately 0.019 G. This circular region contains ($N=$)613 Si-O bonding sites. Assuming that all empty sites can be occupied with equal probability, which corresponds to the random distribution model, one would ideally like to include in the m-electron histogram the frequency spectrum for each possible spatial configuration of m-electrons. Although this was in fact done for one- and two-electron systems, it becomes computationally time prohibitive for more than 2 or 3 electron systems. Thus for 3 or more electron systems, we generated the m-electron histograms using a Monte Carlo method in which the sites for each electron configuration were picked randomly. Each m-electron histogram, denoted as $H_m(\nu)$, is the result of accumulating the resonant frequencies and their corresponding intensities for 100000 m-electron ($m=3,4,5$) configurations; w_m denotes the number of configurations in the m-electron histogram. For the six-electron configuration, our plots were based on data taken with 20440 configurations. This gives an estimated uncertainty in the calculated dipolar linewidth of less than 2%.

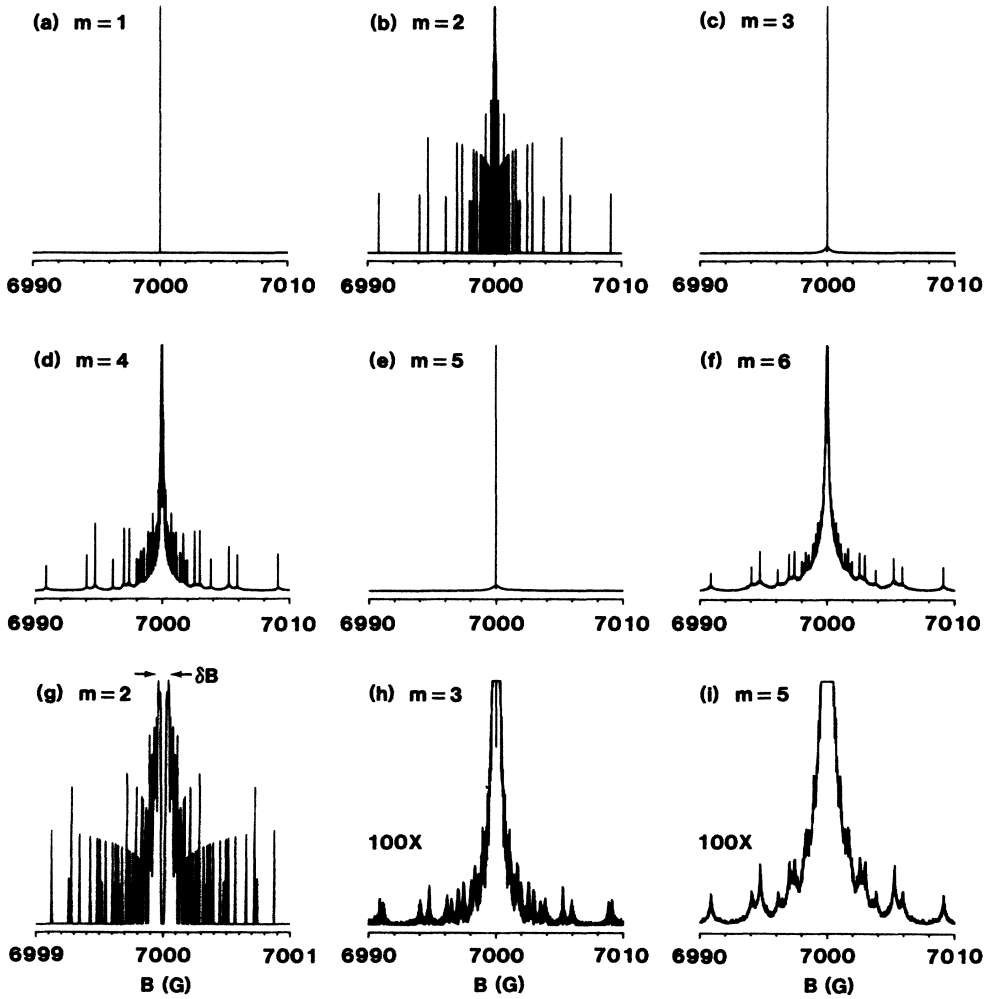

FIG. 7. (a) Histogram for the Zeeman resonance. (b)—(f) Histograms for the 2-, 3-, . . ., and six-electron systems. (g) Histogram for the two-electron system very near 7000 G; δB is defined in Eq. (9). (h) and (i) Vertical scale for the odd-electron systems amplified by a factor of 100 showing details in the satellite structure for the three- and five-electron systems.

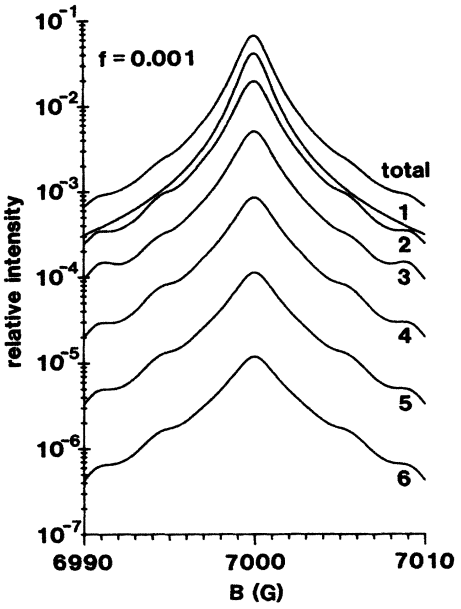

FIG. 8. Semilog plot of the dipolar histogram spectra convoluted with a Lorentzian function having a linewidth [full width at half maximum (FWHM)] of $(3)^{1/2}$ G for each of the 1-, 2-, . . ., 6-electron systems with intensity resulting from a fractional site occupancy of 0.001.

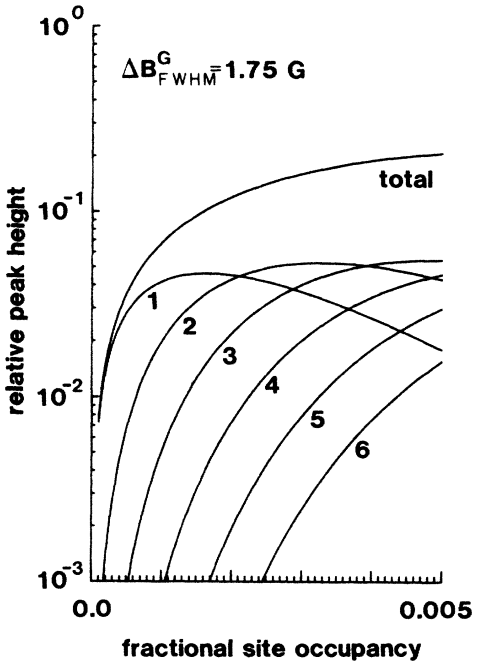

FIG. 9. Plot of the peak height of a dipolar spectra convoluted with a Gaussian function as a function of fractional site occupancy. This plot shows the relative importance of the contributions from the various many-electron configurations.

The total dipolar histogram for a given fractional site occupancy parameter f is $H_{\text{total}}(\nu)$ where

$$H_{\text{total}}(\nu)=\sum_{m=1}^{p} U_m V_m H_m(\nu) . \tag{10}$$

The term U_m is the normalizational factor for the m-electron configuration where

$$U_m=\frac{N!}{m!(N-m)!w_m} , \tag{11}$$

and V_m is the statistical weight factor which is given by

$$V_m=f^m(1-f)^{N-m} . \tag{12}$$

The line shapes of the spectra for each of the m-electron systems convoluted with a Lorentzian function to approximate the effects of other sources of line broadening are illustrated in Fig. 8.[22]

The final results of this calculation are shown in Figs. 9–11. In order to include the effects of ^{29}Si hyperfine broadening, each of the m-electron histograms representing dipolar broadening are convoluted with a Gaussian function which is intended to be representative of ^{29}Si hyperfine broadening.[23] The relative importance of the various m-electron configurations in the dipolar broadening of the total resonance as a function of the fractional site occupancy is shown in Fig. 9. The results in Fig. 9 show that in order to obtain convergence for fractional site occupancies approaching 0.005 for a region 100 Å in diameter, one needs to admix spectra of at least up to six-electron systems.

The full width at half maximum (FWHM) linewidth due to the dipolar broadening convoluted with a Gaussian line-broadening function is shown in Fig. 10 as a function of the fractional site occupancy f. A Gaussian linewidth of $\Delta B^G_{\text{FWHM}}=1.75$ G was chosen so as to match the total

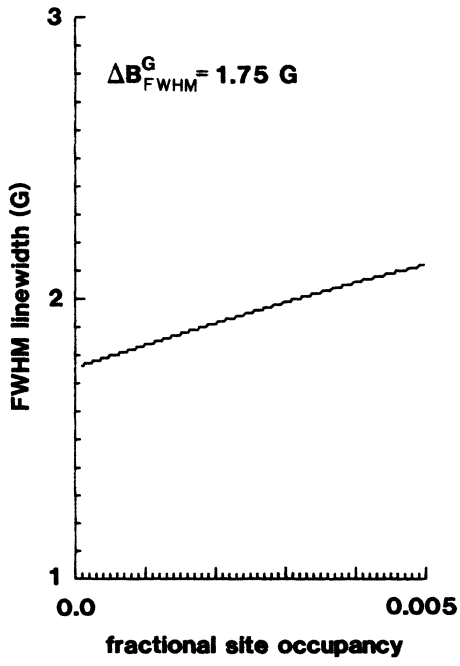

FIG. 10. Plot of the FWHM linewidth as function of fractional site occupancy which shows the added contribution due to dipolar interactions.

FWHM linewidth observed experimentally. The results in Fig. 10 indicate that the contribution to the overall linewidth due to dipolar effects is rather small—approximately 0.35 G for $f=0.005$.

The calculated line shape for $f=0.005$ is shown in Fig. 11(a); here one can see the resolved fine-structure resonances due to 5NN (labeled *e*, 6 equivalent sites, 11.5-Å pair separation), 6NN (labeled *f*, 6 equivalent sites, 13.3-Å pair separation) and 7NN (labeled *g*, 12 equivalent sites, 13.8-Å pair separation) pairs. The calculated line appears more Gaussian than the measured resonance shown in Figs. 2(b) and 11(b), which is mostly Lorentzian.

In the case of the measured resonance in Fig. 11(b), one observes a pair of resolved satellite resonances. The question is whether these observed satellite lines are ^{29}Si hyperfine lines or fine-structure resonances. The relative intensity in these two satellite lines is 1.95 and the relative intensity of the main resonance is 20.1. If they were ^{29}Si hyperfine lines arising from 3 equivalent sites, the ratio of the satellite intensity to that of the main line would ideally be 0.148. The observed ratio is 0.097. The effects of strain can cause an apparent loss of measureable hyperfine intensity.[7] However, the intensity of the observed satellite lines is obviously significantly more than that of the individual, calculated fine-structure resonances in Fig. 11(a).

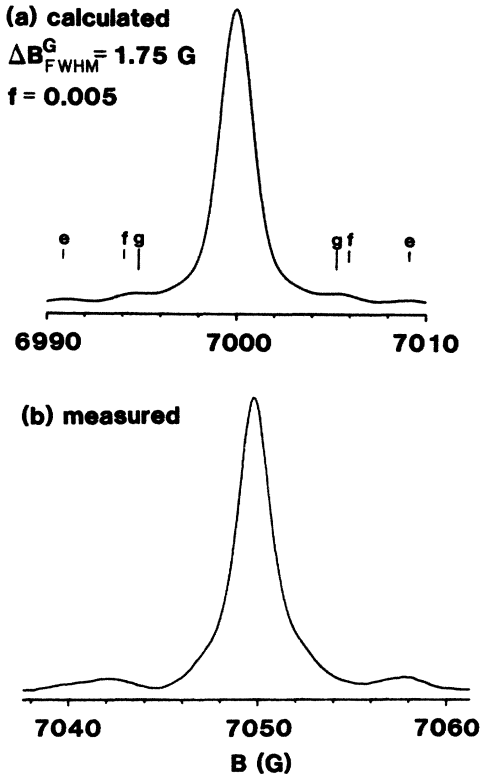

FIG. 11. (a) Calculated spectrum resulting from convoluting the dipolar histograms with a Gaussian function representing other line-broadening effects. The pairs of satellite lines indicated by *e*, *f*, and *g* correspond to fine-structure pair lines arising from 5, 6, and 7 nearest-neighbor dangling-bond pairs. The measured spectrum is shown in (b) for comparison.

This evidence more strongly supports the interpretation that the observed satellite lines are due to ^{29}Si hyperfine interactions. The slight flattening at the base of the main resonance also appears to be due to nearly unresolved satellite structure.

The overall result obtained from this computational approach is that the linewidth of the observed P_b resonance for **B** perpendicular to the (111) Si-SiO_2 interfacial plane *is* consistent with hyperfine and electronic dipolar broadening effects. Unfortunately, the contribution due to dipolar broadening is small under the optimistic assumptions used in this computational model and is not sufficiently large to enable us to deduce information about the distribution of the dangling bonds. Although the method of moments has been of great importance in the analysis of numerous resonance lines, there may be other cases such as this one in which it is inadequate.

IV. SUMMARY AND CONCLUSIONS

The existence of dangling bonds directed only along the [111] direction perpendicular to the (111) Si-SiO_2 interface has been interpreted to mean that these unpaired electrons are localized on Si atoms associated with the crystalline Si at the silicon "surface" of the interface which are not bonded to an oxygen atom which forms the abrupt transition to the oxide.[6] Transmission-electron-microscopy studies of the samples used in our EPR studies of the (111) Si-SiO_2 interface indicated that this interface was atomically flat to within 2 (111)-plane spacings over long distances. Atomic steps at the interface ranged in spacing from 15—300 Å with an average step spacing of $\approx$110 Å. EPR measurements indicated that the surface density of dangling bonds (P_b centers) in these samples was between 3 and 5×10^{12} cm^{-2}. This corresponds to a fractional site occupancy of between 0.004 and 0.006.

The surface spin density is such that perhaps the effects of interactions between the unpaired electrons might be observable in our EPR spectra. Such interactions could conceivably provide additional information concerning the spatial distribution of dangling bonds at the interface and possibly be relevant to the question regarding the physical mechanism(s) by which these defects are created. Close examination of the EPR spectra have failed to identify any resolved fine-structure spectra due to pairs of dangling bonds with a pair separation of <13 Å. We suggest three possible reasons as to why resolved fine-structure lines might not be observable: (1) Isotropic exchange interactions for close pairs of P_b centers result in the pair being in a spin singlet state. (2) The planar distribution of P_b centers on the (111) Si-SiO_2 interface is not random but instead is such that the separation between dangling bonds tends to be enhanced. Such a distribution might occur if dangling bonds are created as a result of the release of strain energy from a finite region of the interface during the cool-down period after thermal oxidation. (3) The P_b centers are not confined to a plane but are distributed in depth as well and consequently the probability for close pairs is reduced below our threshold for detection. Although the first two explanations are plausible, the third deduction is inconsistent with the

present model for the P_b center on the (111) Si-SiO_2 interface.

Interactions between dangling bonds separated by more than about 15 Å should also affect the linewidth and possibly the line shape of the main P_b Zeeman resonance. Assuming that exchange effects are insignificant between these more distant pairs, we have examined the effects of magnetic dipole-dipole interactions between unpaired electrons on the main Zeeman line. Although we attempted to define the linewidth and line shape in terms of even moments using the method developed by Van Vleck, we found this method inadequate since we were unable to discriminate between contributions to the moments associated with the resolved and unresolved portions of the total spectrum.

In our final analysis, the effects of dipolar broadening were determined by calculating the dipolar spectra by a Monte Carlo method for various spatial configurations of 1, 2, . . ., 6 electron systems confined to a finite region. The result of this computational approach is that the linewidth of the observed P_b resonance for **B** perpendicular to the interface is consistent with ^{29}Si hyperfine and electronic dipolar broadening effects. The contribution to the total linewidth (2.1 G FWHM) due to dipolar effects alone is only about 0.35 G. Consequently, the small contribution to the linewidth from dipolar effects, which should have an angular variation similar to that shown in Fig. 6, has proved to be too small to detect.[8]

Note added in proof We have recently learned that J. Braet has also performed moment calculations on this problem. [J. Braet, Ph.D. thesis, Katholieke Universiteit Leuven (1985)].

ACKNOWLEDGMENTS

Appreciation is expressed to James Knapp who lent us the use of his Hewlett-Packard HP9817 desk-top calculator in the off hours for many of the calculations performed in this paper. This work has benefited from the numerous discussions one of us (K.L.B.) has had with P. M. Richrads, D. K. Brice, S. M. Myers, and A. Stesmans on various aspects of this work. This work was performed at Sandia National Laboratories and supported by the U.S. Department of Energy under Contract No. DE-AC04-76DP00789.

[1]O. L. Krivanek, D. C. Tsui, T. T. Sheng, and A. Kamgar, in *The Physics of SiO_2 and its Interfaces,* edited by S. T. Pantelides (Pergamon, New York, 1978), p. 356.

[2]J. H. Mazur, R. Gronsky, and J. Washburn, Proc. Soc. Photo-Opt. Instrum. Eng. **463**, 88 (1984).

[3]J. H. Mazur and J. Washburn, in *Proceedings of the Physics of VLSI,* AIP Conf. Proc. No. 122 edited by J. C. Knight (AIP, New York, 1984), p. 52.

[4]F. A. Ponce and T. Yamashita, Appl. Phys. Lett. **43**, 1051 (1983).

[5]E. H. Poindexter, E. R. Ahlstrom, and P. J. Caplan, in *The Physics of SiO_2 and its Interfaces,* edited by S. T. Pantelides (Pergamon, New York, 1978), p. 227.

[6]P. J. Caplan, E. H. Poindexter, B. E. Deal, and R. R. Razouk, J. Appl. Phys. **50**, 5847 (1979).

[7]K. L. Brower, Appl. Phys. Lett. **43**, 1111 (1983).

[8]K. L. Brower, Phys. Rev. B **33**, 4471 (1986).

[9]P. M. Lenahan and P. V. Dressendorfer, Appl. Phys. Lett. **41**, 542 (1982).

[10]E. H. Poindexter, G. J. Gerardi, M.-E. Rueckel, and P. J. Caplan, J. Appl. Phys. **56**, 2844 (1984).

[11]K. L. Brower, in *Thirteenth International Conference on Defects in Semiconductors,* edited by L. C. Kimerling and J. M. Parsey, Jr. (The Metallurgical Society of AIME, Warrendale, PA, 1985), p. 485.

[12]K. L. Brower, Radiat. Eff. **8**, 213 (1971).

[13]J. N. Lomer and A. M. A. Wild, Radiat. Eff. **17**, 37 (1973).

[14]Y.-H. Lee and J. W. Corbett, Phys. Rev. B **13**, 2653 (1976).

[15]K. L. Brower, Phys. Rev. B **4**, 1968 (1971).

[16]G. D. Watkins, Phys. Rev. **155**, 802 (1967).

[17]J. H. Van Vleck, Phys. Rev. **74**, 1168 (1948).

[18]C. Kittel and E. Abrahams, Phys. Rev. **90**, 238 (1953).

[19]J. W. Orton, *Electron Paramagnetic Resonance* (Gordon and Breach, New York, 1968), p. 75.

[20]The computations presented in this paper were performed with three Hewlett-Packard HP9816/9817 desk-top computers. The programs were written in PASCAL, compiled, and executed using a floating-point arithmetic board for maximum computational speed. In the case of the six-electron program, the large number of program coding statements specifying the Hamiltonian matrix elements and transition probability matrix elements was systematically generated by a PASCAL code generator program, and this generated code was incorporated into the six-electron program.

[21]The transformation used was $B = h\nu/\mu_B g$.

[22]In order to present the line shapes assoicated with all the electron configurations on a semilog plot, it was necessary to use a Lorentzian function, which has long tails, rather than a Gaussian function in the convolution of the dipolar histograms.

[23]H. Seidel and H. C. Wolf, in *Physics of Color Centers,* edited by W. Beall Fowler (Academic, New York, 1968), p. 557.

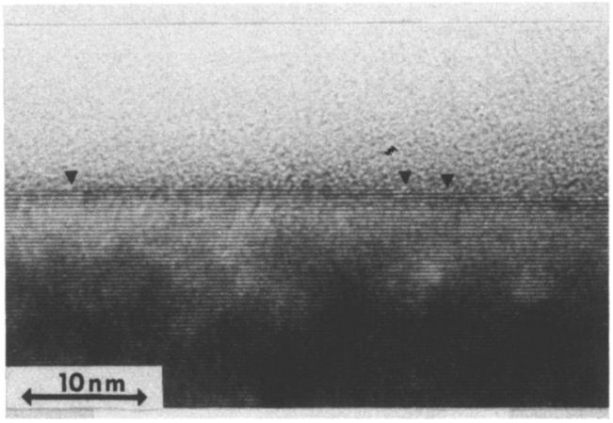

FIG. 3. Transmission electron microscopy view of the (111) $Si-SiO_2$ interface on samples selected at random from the original group from which other samples had been selected for EPR measurements. The samples in the "original group" were all thermally oxidized at the same time. The arrows indicate the positions of ledges or steps at the interface.